Available online at www.sciencedirect.com
SCIENCE DIRECT®
Prog. Polym. Sci. 30 (2005) 915–938
PROGRESS IN POLYMER SCIENCE
www.elsevier.com/locate/ppolysci

# Mechanical performance of polymer systems: The relation between structure and properties

Han E.H. Meijer*, Leon E. Govaert

*Materials Technology, Dutch Polymer Institute, Eindhoven University of Technology, W-hoog 4.140, P.O. Box 513, 5612 MB Eindhoven, The Netherlands*

Accepted 24 March 2005

**Abstract**

A direct relation between molecular characteristics and macroscopic mechanical properties of polymeric materials was subject of a vast number academic and industrial research studies in the past. Motivation was that an answer to this question could, in the end, result in guidelines how to construct tailored materials, either on the molecular level or, in heterogeneous materials, on the micro-scale, that could serve our needs of improved materials without the need of extensive trial and error work. Despite all attempts, no real universally applicable success was reported, and it was only after the introduction of the concept of the polymer's intrinsic deformation behavior that some remarkable progress could be recognized. Thus, it is first important to understand where *intrinsic* deformation behavior of polymeric materials stands for. Second, it is interesting to understand why this intermediate step is relevant and how it relates to the molecular structure of polymers. Third and, in the end, the most computational-modeling-based question to be answered is how intrinsic behavior relates to the macroscopic response of polymeric materials. This is a multi-scale problem like encountered in many of our present research problems.


*Keywords:* Amorphous polymers; Toughness; Intrinsic behavior; Mechanical properties; Constitutive modeling; Multi-level finite element method; Structure–property relations

**Contents**



* Corresponding author.
*E-mail address:* h.e.h.meijer@tue.nl (H.E.H. Meijer).
*URL:* www.mate.tue.nl.

0079-6700/$ - see front matter © 2005 Published by Elsevier Ltd.
doi:10.1016/j.progpolymsci.2005.06.009

## 1. Introduction

Bridging the gap between molecular and macroscopic properties, with as extra intermediate step the processing history, see Fig. 1a, is a just as challenging as impossible task. Reason is that the multi-scale problems involved require far too much computational time and computational memory to be resolved via ab initio analyses. Analyses on different scales require averaging the resulting properties from the analysis on the underlying scale, consequently loosing detail. Therefore, alternatives are searched for. A big step forward was made with the development of a video-controlled tensile test by Christian G'Sell at the Ecole des Mines in Nancy [1,2]. This technique enabled the experimental assessment of the intrinsic deformation behavior: the polymer's stress response measured during homogeneous deformation. More or less simultaneously, Mary Boyce, at MIT, optimized the much more practical uniaxial and plain strain compression tests to obtain similar information in different loading geometries [3,4]. Reason to be pleased with this intermediate step is twofold. **First,** our present

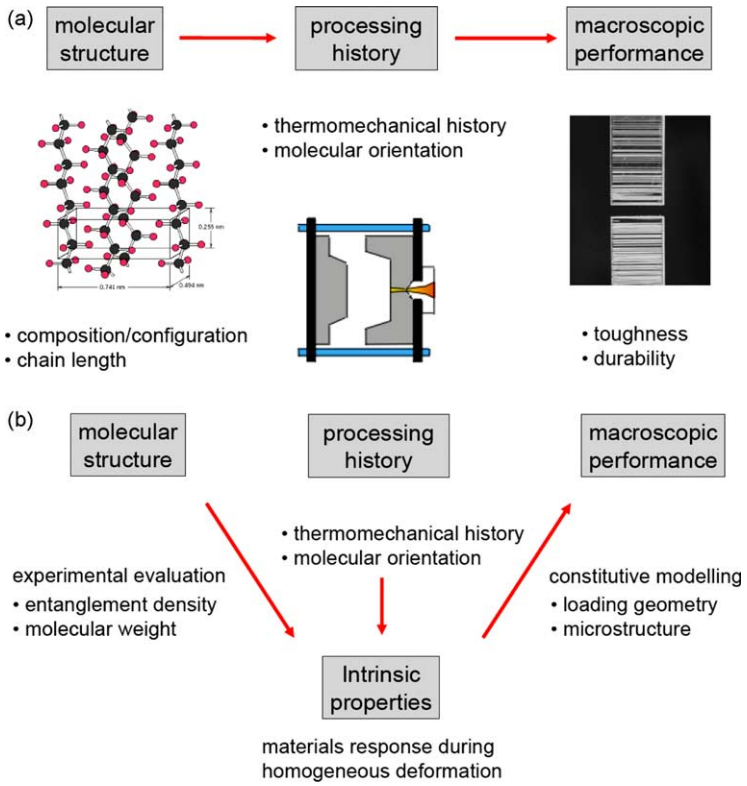


Fig. 1. From molecular details to macroscopic response via the intermediate of the polymer's intrinsic deformation.

advanced computational tools and expertise can be successfully used in the relation between the intrinsic behavior and the macroscopic response, the right-hand side of Fig. 1b. Prerequisite for the success of this route was the development of constitutive models that could capture the intrinsic behavior. So let start to focus on this issue. It is known that it took the polymer melt rheology community some half a century to arrive at constitutive equations that are not only valid in simple shear flows but also can deal with extensional flows. The (extended) Pom Pom model quantitatively describes the melt rheology for branched, and even also for linear, polymers, in complex flows and is based on molecular characteristics [5–7]. Since rheology is based on fluid mechanics, rheologists can be considered as successors of Isaac Newton, thus mathematically educated scientists. Therefore, it is at least remarkable that it took them that much time. The main topics of the rheologist's concern were the quantitative modeling of the deformation rate dependent shear and elongational viscosity and first (and eventually second) normal stress difference, in *incompressible homogeneous* time dependent start-up flows. Interesting now is that the major problem encountered in the solid state rheology of the same polymers is that they are per definition tested in *compressible inhomogeneous* start-up flows in extension. Solid state rheologists can be considered as the successors of Robert Hooke. They are practical engineers that have to deal with the impossible interpretation of the most widely used test: the tensile test on a normalized dogbone-shaped sample that, at best, shows only a simple localization behavior, like necking. All relatively recent progress reported in solid state rheology made of course use of the results obtained in the constitutive equations for melts and the good news is that at present the macroscopic response of amorphous polymers to shear and tensile loading can now be quantitatively described. In plain strain 2D, or even in completely 3D computations, in short and in long time loading, in homogeneous and also in heterogeneous systems, once the polymer's intrinsic behavior (and its microstructure in case of heterogeneous systems) is known. Use is made of standard (e.g. Marc, Abaqus) software combined with custom made (Multi-Level-Finite-Element) analyses.

**Second,** the relation between molecular properties of polymers and their intrinsic behavior, the left-hand side of Fig. 1b, are accessible via well defined experiments that are much easier interpretable than when compared to the results of tensile tests, creep and fatigue tests or Izod impact tests. So let us focus now on the structure of polymers.

## 2. Structure of polymers

Polymers are different from other construction materials like ceramics and metals, because of their macromolecular nature. The covalently bonded, long chain structure makes them macromolecules and determines, via the weight averaged molecular weight, $M_w$, their processability, like spin-, blow-, deepdraw-, generally melt-formability. The number averaged molecular weight, $M_n$, determines the mechanical strength, and high molecular weights are beneficial for properties like strain-to-break, impact resistance, wear, etc. Thus, natural limits are met, since too high molecular weights yield too high shear and elongational viscosities that make polymers inprocessable. Prime examples are the very useful poly-tetra-fluor-ethylenes, PTFE's [8,9], and ultra-high-molecular-weight-poly-ethylenes, UHMWPE's [10], and not only garbage bags are made of poly-ethylene, PE, but also high-performance fibers [11–13] that are even used for bullet proof vests (alternatively made from, also inprocessable in the melt, rigid aromatic polyamides [14,15]). The resulting mechanical properties of these high performance fibers, with moduli of 150 GPa and strengths of up to 4 GPa, represent the optimal use of what the potential of the molecular structure of polymers yields, combined with their low density. Thinking about polymers, it becomes clear why living nature used the polymeric concept to build its structures. And not only in high strength applications like wood, silk or spider-webs.[1]

[1] About nature's processing: What is the melting point of ceramics? And that of metals? If these materials are to be processed at ambient temperature and atmospheric pressure, then what is their solubility? How does nature use chemistry to make teeth and bones? Most of this is known and, interestingly, comes rather close to techniques we use in polymer technology.

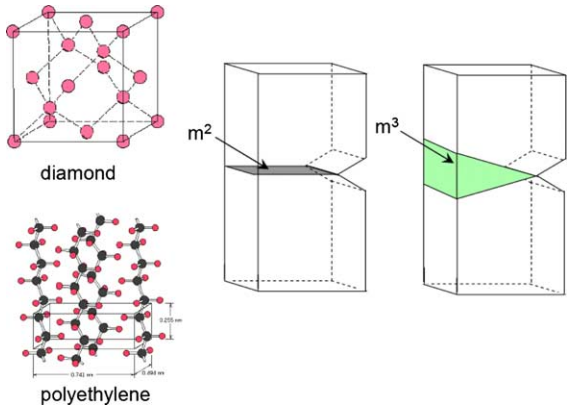


Fig. 2. Diamond, PE and the notched impact test.

Let us now consider diamond, a covalently bonded structure of carbon atoms. What is the energy to create new surfaces in diamond, known as the strongest material in nature? The answer is 1 J/m$^2$. How much is that? It is the energy that comes free if '*an ordinary apple falls from an ordinary table*' [16]. And that is shocking, especially because in this *experiment* we splitted the two surfaces at once, without applying any zipping process. It is the interaction potential that quantifies the energy needed to split atoms, and thus also to create ideal surfaces made of those atoms. How thus this explain the impact toughness of a standard, commodity polymer like PE, which is chemically spoken diamond with two out of the four strongest bonds in nature (covalent) replaced by two of the weakest bonds (Van der Waals), and that measures, in a standard Izod impact test, a value of $10^5$ J/m$^2$? The answer to this question is delocalization. If a material is able to delocalize its strain, out of the area of the largest stress, it will undergo deformation in the volume. This volume deformation is, in a standardized test like Izod-impact, still attributed to the geometrical cross-sectional area in the test bar, behind the notch, see Fig. 2.[2]

In the glassy state the polymer's secondary bonds determine the elastic part of the mechanical properties, modulus and yield stress, while the primary bonds in the network potentially induce the necessary delocalization of local strain that gives toughness. Given this mechanism we conclude that all amorphous polymers with a $T_g$ above room temperature have roughly the same elastic Young's (not Hooke's[3]) modulus of 3 GPa. Low, compared to both competitors, ceramics and metals, since controlled by their weak secondary bonds. Even worse becomes the case for semicrystalline polymers with a $T_g$ below room temperature, that should be considered as a gel of an amorphous fluid physically kept together by higher melting crystals. Only in high performance fibers, like UMWPE and aromatic polyamides, the covalently bonded structure is mechanically addressed during loading, provided that sufficient length is given to the weak secondary interactions to transfer the load from one molecule to the other. This, of course, only works in the direction of the processing-induced 100% main chain orientation. Non-oriented polymers basically only strongly differ in impact strength or, equivalently, their ability to delocalize strain. Ceramics are intrinsically brittle but some are less brittle, like man-made ceramic fiber reinforced ceramics [17] or the natural multi-layered tooth or seashell ceramics [18,19], the last with typically 400 nm sized layered structures. Delocalization in the artifacts is realized because the ceramic fibers survive the breaking and bridge the cracks, giving rise to both a second dissipation mechanism via debonding along the fibers and in the end a possibly local strain hardening via cooperative fiber loading. This is also the way stone reinforcement in concrete works. Delocalization in the natural objects is induced by weakening the structure perpendicular to the loading direction yielding a multiple cracking mechanism, see Fig. 3. This principle is comparable to the change of diamond into

[2] We should define impact values only in J/m$^2$. Either or not correct, volume deformation is attributed to the surface energy. A value of 100.000 J/m$^2$ for PE is of course rather arbitrary. It represents the maximum energy absorbed in the (optically stress-whithening) volume during polymer testing using the Izod test-bar, and it is partly determined by the sample geometry. A value like that for PE means in practice: no-break.

[3] 'The power of any springy body is in the same proportion with the extension (Sic vis, sic extensio)' was Hooke's way in 1676 to express the constitutive equation for a solid that we now write as $\sigma = G\gamma$, or $\boldsymbol{\sigma} = G\,\mathbf{B}$ in 3D, where Newton's 1687 definition of the viscosity for fluids was 'The resistance which arises from the lack of slipperiness of the parts of the liquid, other things being equal, is proportional to the velocity with which the parts of the liquid are separated from one another', that we now write as $\sigma = \eta\dot{\gamma}$, or $\boldsymbol{\sigma} = 2\eta\,\mathbf{D}$ in 3D.

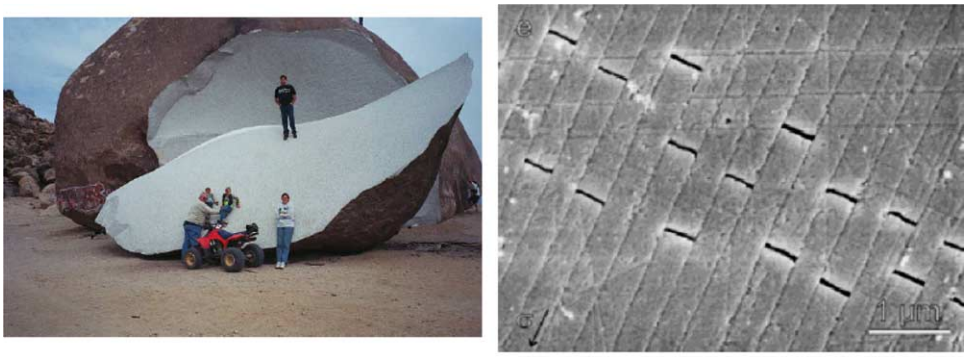


Fig. 3. Breaking of homogeneous (left) and heterogeneous (right) ceramics. The figure on the left shows catastrophic strain localization in a Californian Giant Rock induced by thermal stresses from a nightly fire. The figure on the right shows delocalized strain in seashell ceramics, see Refs. [18,19].

polyethylene, weakening the structure in some directions, thus suffering in mechanical bulk behavior like modulus and yield strength and, where seashells are still pretty hard and strong, polyethylene will never be diamond anymore.

## 3. Intrinsic deformation

Our basic question was: where does the intrinsic behavior of polymers originate from and can we understand it? To answer that, we start with returning to the original work of Haward and Thackray of 1965 who described the material's response with two parallel processes: (i) the initial non-linear elastic response up to yield, controlled by the secondary, intermolecular, interactions, combined with (ii) the entanglement network response in parallel from the primary intramolecular interactions which gives an entropic contribution at large strains [20]. In Hawards' approach, see Fig. 4, the secondary interactions were modeled via a Maxwell model (fluid!), where all non-linearity was put into the stress-activated viscosity function that followed an Eyring model. The original model not only received a typical polymer type of response in terms of citations with a change in slope from 1 to 3 at the onset of the use of continuum mechanics based computer modeling [21], but also basically was at the cradle of the solid state rheology. Its conceptual approach was followed and

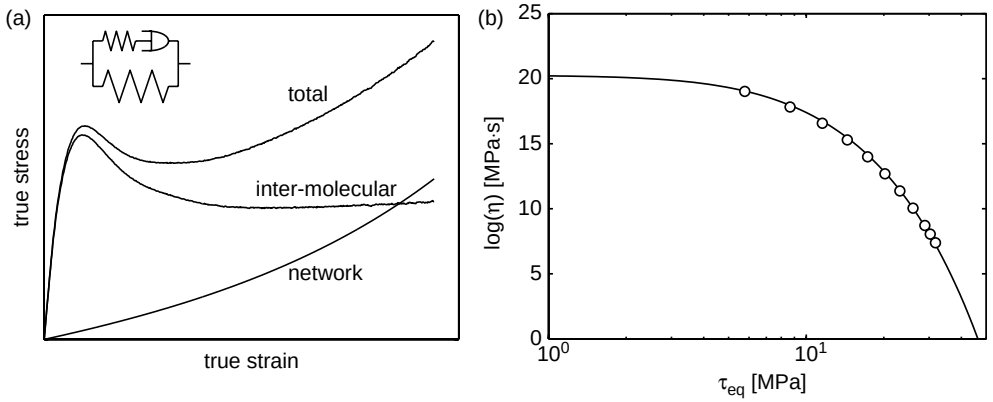


Fig. 4. The stress decomposition proposed by Haward and Thackray [20] (a). For its present 3D formulation, see Table 1. Further we show the characteristic stress-dependence of the viscosity of the dashpot for PC at room temperature [27] (b).

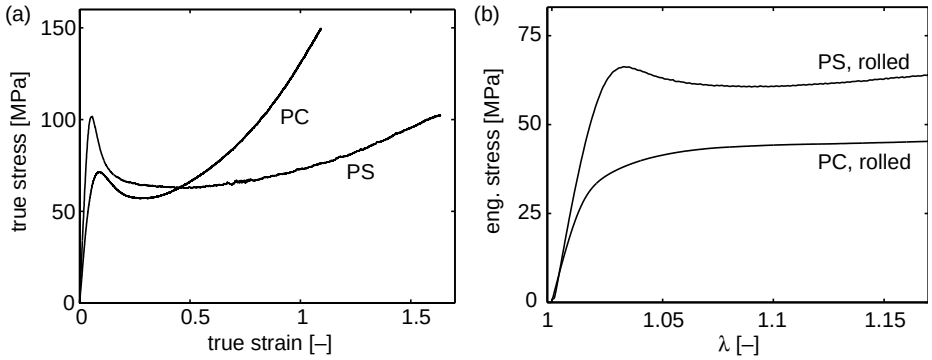


Fig. 5. Intrinsic behavior of polycarbonate PC and polystyrene PS before (a) and after (b) mechanical rejuvenation.

extended to full 3D constitutive relations by several research groups, e.g. those of Mary Boyce at MIT [3,22,23], Paul Buckley in Oxford [24–26] and our group at the TU/e in Eindhoven [27–29]. Common factors in these models are the application of rubber elasticity to model strain hardening and a stress-dependent viscosity to capture the deformation kinetics. Similar to temperature, an applied stress leads to an increase in segmental mobility [30,31] with a resulting decrease in viscosity; in extreme this leads to yielding, the onset of flow, induced by stress (stress-induced glass transition). In the case of polycarbonate, PC [27] an equivalent stress of 30 MPa lowers the viscosity of the material with 12 decades (see Fig. 4b)!

Knowing that for atactic polypropylene, PP,[4] ab initio calculations by Doros Theodorou and Uli Suter, at that time at MIT, showed that affine deformations along the chain do not exists outside a region of roughly 10 C-atoms [32], we can still today conclude that the process of plastic deformation in amorphous polymers is controlled by molecular motions on a segmental scale. Thus molecular weight and entanglements should not play a dominant role. Only the secondary interactions and the free volume kinetics could be of primary interest. Once the critical stress is surpassed, the stress to further flow should be constant, until the entanglement network starts to orient, manifesting itself in strain hardening (represented by the parallel spring in the Haward model). Here, it is the entanglements that control the modulus and it is the molecular weight that controls the strength at breakage. In this picture there seems to be no reasoning for strain softening. This now is somewhat more important than its first glance seems to be, see Fig. 5.

The combination of strain softening, after yield, followed by strain hardening, at larger deformations, proves to be the key issue in understanding mechanical behavior. Their mutual ratio determines whether a polymer will manifest non-catastrophic localization (like in bullet-proof polycarbonate PC), or will show catastrophic localization in terms of craze formation perpendicular to the loading direction (like in the brittle polystyrene PS) [33]. The origin of strain softening thus seems to be important and it was only after reaching an extreme intrinsic behavior that some progress was realized. What is extreme behavior? Basically, it is the response of a completely fresh material. Best way to realize that state is by mechanical rejuvenation, rather than by applying thermal rejuvenation[5] (that are not identical [34]). This is the best illustrated by the fact that the lowest yield stress reached via thermal rejuvenation in PC is approximately 57 MPa, while mechanical rejuvenation of PC at sufficiently high strains ($\gamma = 0.3$) yields 35 MPa.[6] In PC, mechanical rejuvenation can be

[4] The only polymer that at that time could properly be modeled since it did not suffer from either large geometrical hindrance (like in polystyrene PS) or from polar interactions (like in polyvinylchloride PVC), neither did it crystallize.

[5] Melting followed by fast quenching to the solid state is referred to as thermal rejuvenation.

[6] Discussions on whether mechanical rejuvenation is the same as thermal rejuvenation still continue. The answer is simple: It is not, because mechanical rejuvenation is superior, since during the quench in thermal rejuvenation, the polymer starts to considerably age already.

achieved by twisting a cylindrical test bar to and fro over 720° at room temperature prior to tensile testing [35]. For lower entanglement density polymers like PS this does not work (crazes occur) and an alternative route was explored in deforming the material at room temperature under (compressive) stresses via a 30% height reduction in a two-roll milling process [36,37]. For PC, 10% proves to be sufficient to induce homogeneous deformation without neck formation. Also, PS shows homogeneous deformation, without neck, but also without craze formation, see Fig. 6.

Our understanding is that once the secondary bonds are locally weakened by stress, the material must flow under a constant stress up to the point that strain hardening sets in. And that is exactly what we find in rejuvenated materials. During the cold rolling process we pushed the original, aged, material to a strain that was sufficiently large that we entered the start the strain hardening part of the intrinsic deformation curve. By the way, interestingly enough, the density of the polymers increased during this process of mechanical rejuvenation. After release of the stress and reloading, the yield stress proved to be reduced to the extent that no softening occurs anymore. The cause of strain localization is thus removed and that explains the no-necking for PC and the no-crazing of PS. The low yield stress, though, does not remain and in time, ageing time, it increases, leading to a return of softening and thus the return of brittleness. For PS (with its low density thus high free volume, low entanglement density, high chain stiffness and thus high molecular weight between entanglements of about 20.000), brittleness returns within hours after rejuvenation and for PC ($M_e \approx 2000$) it is a matter of months before necking is observed again, see Fig. 7.

In classical free volume theories for ageing, an increase in density is always accompanied with an increase in yield stress. During mechanical

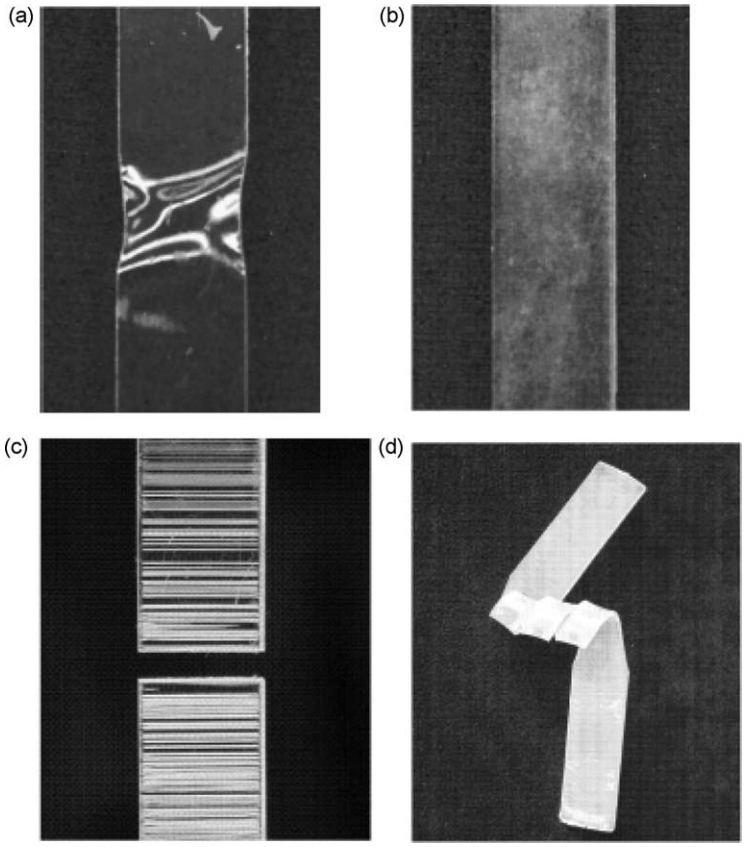


Fig. 6. Deformation in the quenched (a and c) and mechanically rejuvenated state (b and d) for PC (a and b) and PS (c and d) [33].

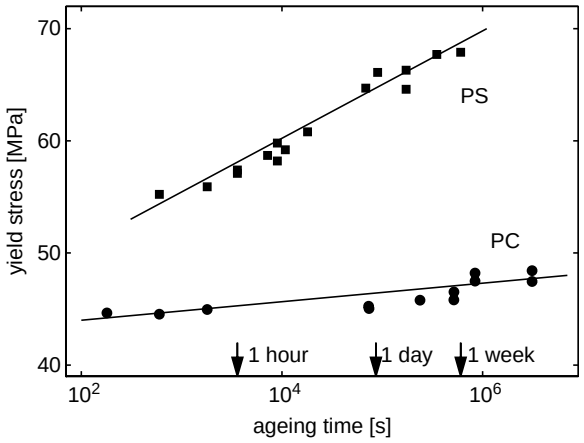


Fig. 7. Increase in yield stress in time upon physical ageing after mechanical rejuvenation.

rejuvenation *the opposite* occurred. Physical ageing experts tried to make the free volume theory the holey Grail of polymer physics. They failed but later explained that they, of course, meant the free volume *distribution* being the responsible driving force [38]. We conclude from our experiments that free volume is just a, let us say, *related property*.

## 4. Physical ageing

What causes the yield stress to increase in time upon ageing? Already in the 1970s it was quantified that upon ageing of amorphous polymers in calorimetry, DSC, a pronounced enthalpy peak develops near the glass transition temperature [39,40]. Simultaneous with the development of this enthalpy overshoot, the yield stress is observed to increase [41,42]. Both effects can be rationalized in terms of an evolution of the potential energy landscape [43–46].

The change in time of the energy landscape, that is the local attraction of individual atoms to their neighbours is illustrated in Fig. 8c and shows a local densification upon physical ageing. Indeed, a free volume *distribution* if you want, but rather a local attraction-energy distribution. In order to induce molecular mobility, this local order has to be destroyed. And that is reflected in the growing peak in the DSC signal, Fig. 8b. If segmental mobility is increased not by temperature, but by stress, than we find a growing peak in stress in the stress–strain curve, Fig. 8a, that we *interpret* as an increase in yield stress followed by softening.

Nevertheless, this last combination introduces localization of strain that can be catastrophic when the ratio softening/hardening becomes overcritical and a tough-to-brittle transition is found.

Once in macroscopic homogeneous deformation, e.g. during mechanical rejuvenation via cold rolling, the minima in the energy landscape are pulled out by stress, the energy landscape is flattened, the yield stress lowered, the material is made ‘fresh’ again and does not show strain softening and, consequently, deforms homogeneously.[7]

Within the constitutive model the changes in the yield stress, as a result of physical aging or mechanical rejuvenation, are captured in the evolution of a single state parameter: $S$. The value of this state parameter indicates how strongly the present situation of the polymer deviates from the reference state, in our case the ‘*fresh*’, mechanically rejuvenated state. Plotting the yield stress versus the logarithm of strain rate, an increase of $S$ basically shifts the curves horizontally towards lower strain rates, see Fig. 9a. At a constant strain rate this results in an increase of the yield stress compared to that of the rejuvenated state.

To capture the evolution of $S$ as a function of time and deformation, it is assumed to consist of two contributions that act independently: $S = S_a R_\gamma$. One is the age of the sample, $S_a$. The other is the contribution of mechanical rejuvenation, $R_\gamma$,[8] that decreases the yield stress with ongoing total applied plastic shear. As a result of plastic deformation the yield stress characteristic shifts back to the reference (rejuvenated) state. In a constant strain rate experiment this leads to a drop of the yield stress with increasing strain and the intrinsic stress–strain curve evolves gradually to that of the rejuvenated state.

Fig. 10a compares the intrinsic response of an annealed and a quenched PC sample. Annealing results in an increase of both modulus and yield stress,

[7] Provided that the classical Considère criterion of 1885 is not met, implying that ratio of yield stress and strain hardening modulus should be smaller than 3 to obtain homogeneous deformation also in the absence of strain softening [33].

[8] Basically a function with an initial value of $R_\gamma = 1$, that decreases towards zero with increasing applied plastic strain.

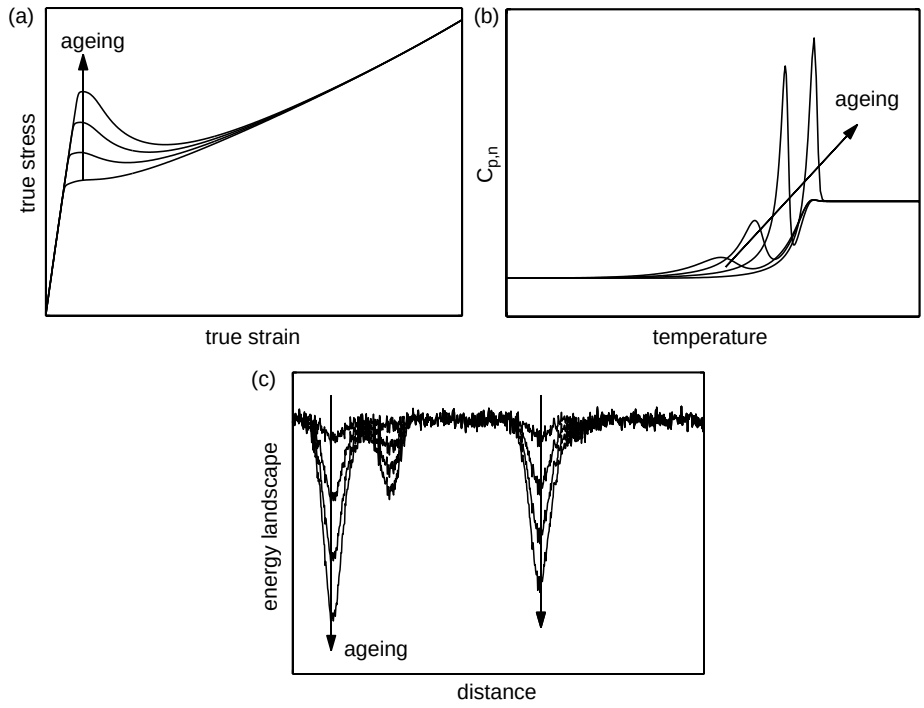


Fig. 8. Increase in yield stress (a) and DSC signal (b) in time upon physical ageing after mechanical rejuvenation and a sketch of the change in energy landscape (c).

but upon plastic deformation the differences between both curves disappear and they fully coincide at a strain of approximately 0.3. All influence of thermal history is erased at that strain and both samples are transformed to the same mechanically rejuvenated state.

From Fig. 10a it is clear that an increase of yield stress, due to a thermal treatment, will directly imply an increase in strain softening. The influence of molecular weight on the intrinsic response is usually small and negligible [29,47], which makes thermal history the key factor in influencing the intrinsic properties of a specific polymer glass.

The influence of progressive physical aging is included through a time-dependent evolution of the

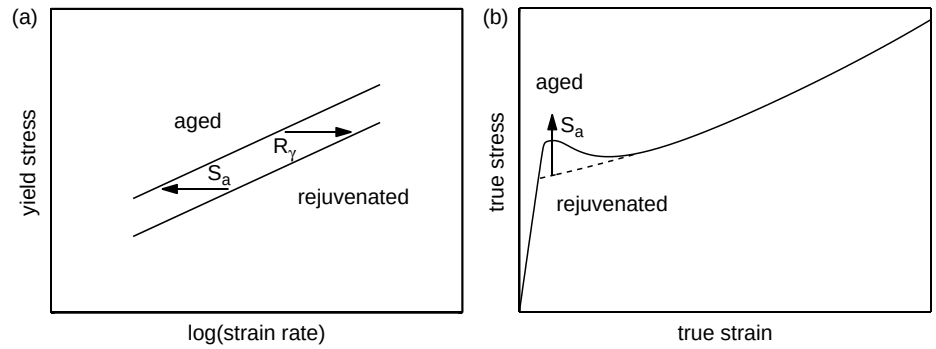


Fig. 9. Schematic representation of the influence of physical aging and strain softening on the strain rate dependence of the yield stress (a). Schematic representation of the intrinsic stress–strain curve indicating the influence of physical aging and strain softening (b).

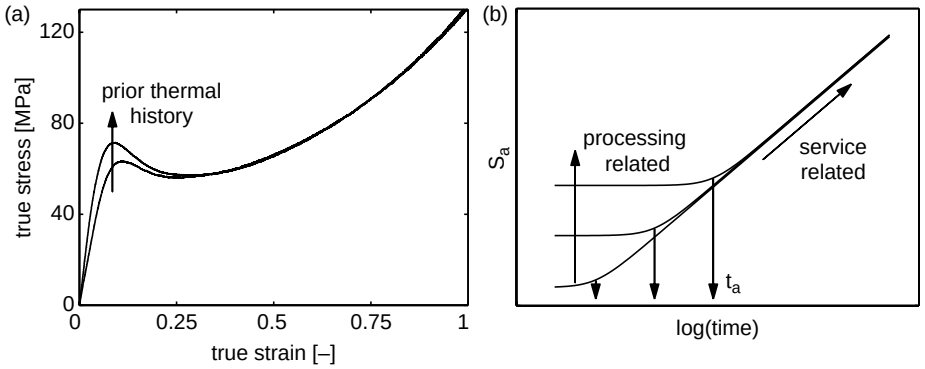


Fig. 10. True stress–strain curves for polycarbonate with two different initial states (quenched and annealed) (a). Schematic representation of the evolution of $S_a$ for different initial states (b).

parameter $S_a$, schematically represented in Fig. 10b. We proposed that the parameter $S_a$ displays a logarithmic evolution in time[9] (see Table 1). The influence of temperature and applied stress are modeled in an effective time approach [29]. For samples with an arbitrary (unknown) thermal history, the determination of the yield stress at a single strain rate is already sufficient to obtain the initial value of $S_a$ and thus to obtain a full, quantitative constitutive description of the material.

## 5. From intrinsic behavior to macroscopic response

The differences between the tough PC and brittle PS are reflected in their intrinsic behavior, see Fig. 5a. The main differences are that in PS the strain softening is more pronounced, while the strain hardening is (much) less. The last is directly related to the entanglement density of PS that is, with an entanglement molecular weight $M_e$ of 20.000 versus 2000 for PC, extremely low. If we just change this entanglement density of PS, simply by mixing with poly-phenylene-ether, PPE (with $M_e$ of 5000), we can increase strain hardening [48] and change the mechanical behavior of PS into that of PC, see Fig. 11.

A more precise investigation on the influence of the intrinsic behavior of polymeric materials on their resulting macroscopic response can now be performed. We start with PC and use a cylindrical test bar, thus allowing for a 2D calculation, with a standard tensile bar shape. Upon loading, we plot the true stress in the mid plane of the bar on different axial positions, see Fig. 12 that shows in cross-section a quarter of the test bar. We conclude that softening after yield results in localization via neck formation, but that the strain hardening in PC is sufficient to make the neck run trough the whole sample, until the diameter increase at the clamping position is reached and the stress in the sample increases until breakage occurs. Next, we compare the intrinsic, true stress–true strain, behavior with the macroscopic engineering stress-engineering strain curve as monitored during testing, see Fig. 13. Fig. 13a plots the stress in the mid plane of the tensile bar where the neck is formed (because we introduced, like in the simulation of Fig. 12, a small imperfection there). In Fig. 13b, the macroscopic, so called stress–strain curve, is plotted as measured on the clamping side of the test bar, see the legend in Fig. 13. We recognize that as soon as yield is past in the intrinsic behavior of Fig. 13a, softening induces a decrease in stress which is reflected as a strong decrease in the engineering stress in the macroscopic part, Fig. 13b. When the neck runs through the macroscopic sample, realized by the intrinsic strain hardening, see Fig. 12, the true stress within the neck remains constant. The length of the plateau found in the macroscopic response of Fig. 13b depends on the sample's geometry, especially the length of the test bar, and thus should never be considered to reflect strain! If

[9] It should be noted that the ageing sensitivity of the yield stress of a polymer is not solely determined by the rate of change of the state parameter $S_a$ (the shift along the strain rate axis), but also by the slope of yield stress versus the logarithm of strain rate.

Table 1
A single-mode 3D, non-isothermal constitutive equation for polymer solids, for explanation and details please download the thesis [29]

| | |
|---|---|
| $\boldsymbol{\sigma} = \boldsymbol{\sigma}_s + \boldsymbol{\sigma}_r$ | $\eta(\bar{\tau}, T, p, S) = \eta_{0,r}(T) \frac{\bar{\tau}/\tau_0}{\sinh(\bar{\tau}/\tau_0)} \exp\left(\frac{\mu p}{\tau_o}\right) \exp(S(t, \bar{\gamma}_\rho))$ |
| $\boldsymbol{\sigma}_s = K(J-1)\mathbf{I} + G\tilde{\mathbf{B}}_e^d$ | $\eta_{o,r}(T) = \eta_{0,r,\mathrm{ref}} \cdot \exp\left[\frac{\Delta U_\gamma}{R}\left(\frac{1}{T} - \frac{1}{T_{\mathrm{ref}}}\right)\right]; \quad \tau_0 = \frac{kT}{V_\gamma^*}$ |
| $\boldsymbol{\sigma}_r = G_r \tilde{\mathbf{B}}^d$ | $S(t_{\mathrm{eff}}(t, T, \bar{\tau}), \bar{\gamma}_p) = S_a(t_{\mathrm{eff}}(t, T, \bar{\tau})) \cdot R_\gamma(\bar{\gamma}_p)$ |
| $\dot{J} = J\,\mathrm{tr}(\mathbf{D})$ | $R_\gamma(\bar{\gamma}_p) = (1 + (r_0 \cdot \exp(\bar{\gamma}_p))^{r_1})^{\frac{r_2-1}{r_1}} / (1 + r_0^{r_1})^{\frac{r_2-1}{r_1}}$ |
| $\overset{o}{\tilde{\mathbf{B}}}_e = (\mathbf{D}^d - \mathbf{D}_p)\tilde{\mathbf{B}}_e + \tilde{\mathbf{B}}_e(\mathbf{D}^d - \mathbf{D}_p)$ | $S_a(t_{\mathrm{eff}}(t, T, \bar{\tau})) = c_0 + c_1 \cdot \log(t_{\mathrm{eff}}(t, T, \bar{\tau}) + t_a)$ |
| $\mathbf{D}_p = \frac{\boldsymbol{\sigma}_s^d}{2\eta(\bar{\tau}, T, p, S)}$ | $t_{\mathrm{eff}} = \int_0^t a_T^{-1}(T(t'))\, a_\sigma^{-1}(\bar{\tau}(t'))\, \mathrm{d}t'$ |
| $\bar{\tau} = \sqrt{\frac{1}{2}\mathrm{tr}(\boldsymbol{\sigma}_s^d \cdot \boldsymbol{\sigma}_s^d)}$ | $a_T(T) = \exp\left[\frac{\Delta U_a}{R}\left(\frac{1}{T} - \frac{1}{T_{\mathrm{ref}}}\right)\right]$ |
| $\bar{\gamma}_p = \sqrt{2 \cdot tr(\mathbf{D}_p \cdot \mathbf{D}_p)}$ | $a_\sigma(\bar{\tau}) = \frac{\bar{\tau}/\tau_a}{\sinh(\bar{\tau}/\tau_a)}; \quad \tau_a = \frac{kT}{V_a^*}$ |

the neck reaches the clamps, the stress starts to increase until breakage occurs in the thinnest section of the bar.

Performing the same analysis on PS, see Fig. 14, we directly recognize that the strain hardening is not sufficient to delocalize the region of the neck. This remains the case even if we do not stop the intrinsic behavior curve but continue to infinity, leading also to infinite stresses within the fibril formed. Even then the deformation remains localized, since the force (the product of the stress times the fibrils cross-section) that the fibril can exert on the remainder of the test bar is insufficient. The stress can go to infinite, the cross-section goes faster to zero. The conclusion is that PS is basically too easy to flow, too ductile to be tough (knowing that toughness is equivalent to delocalization of strain). We now can understand that the arrow in Fig. 1b on the right-hand side can only run in one direction: from intrinsic to macroscopic and it illustrates the difficulty of interpreting macroscopic tests.

## 6. Life time prediction

With the single state parameter $S = S_a R_\gamma$ we were able to predict the polymer's situation from the cradle to the grave. In order to demonstrate this, both the long-term behavior of polymers during static and dynamic loading is investigated as well as the influence of the processing conditions during the formation of the polymer on the development of $S$ and thus on the yield stress. Before starting the long-term loading experiments, the polymer's age is first determined by a single tensile test to find its yield stress which was converted into the present value of $S$. Next, long-term loading tests are performed under

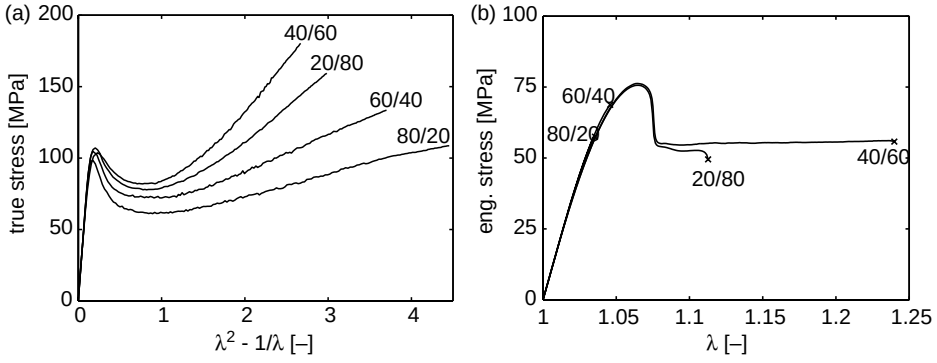


Fig. 11. Noryl® PS–PPE blends in compression (a), and tensile loading (b).

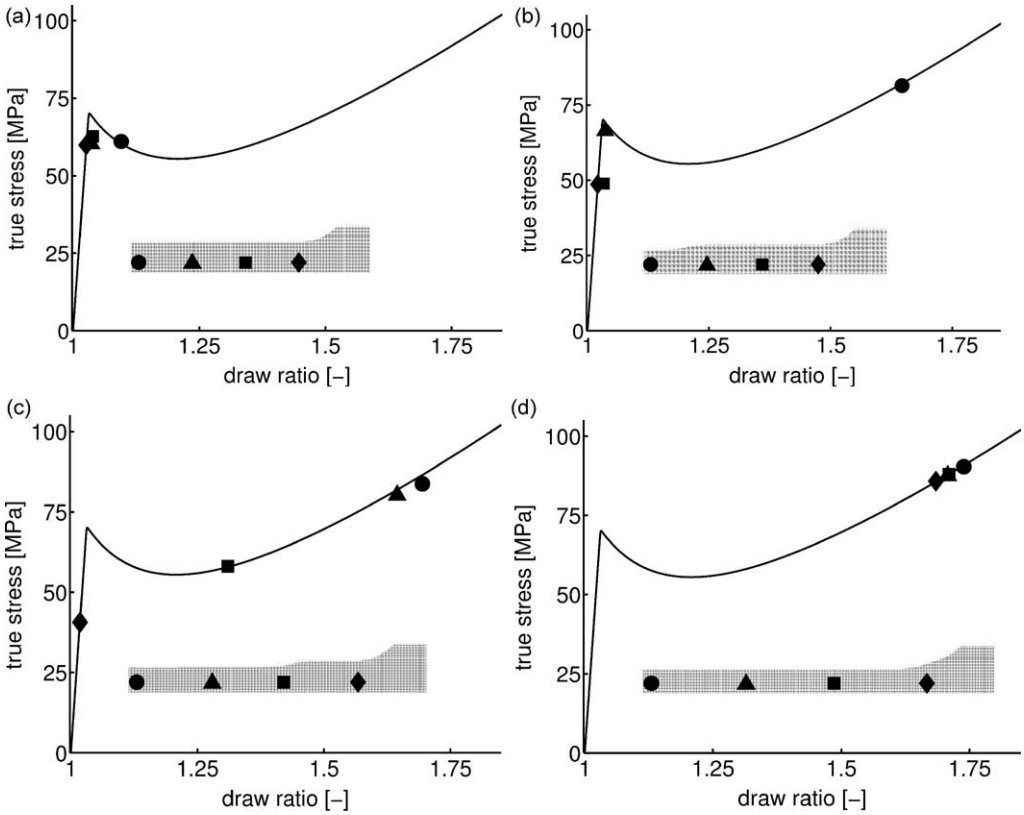


Fig. 12. Tensile testing of PC. After neck formation at yield strain softening sets in, the stress in the remaining part of the test bar decreases substantially due to unloading because of strain localization in the neck. Subsequently, strain hardening occurs in he neck, accompanied by an increase in stress and the neck starts to extend to the whole test bar.

different values of the (constant) stress applied, until creep rupture occurs; see the symbols in Fig. 15a.

Then simulations are performed, the line in Fig. 15a. Because stress-enhanced physical ageing during the tests is incorporated in the simulations, also the endurance limit can be predicted [49]. Remarkable is the accuracy of the predictions that did not use any adjustable parameter. Similar comments can be made on the fatigue loading results, see Fig. 15b.

That was the grave, so how about the cradle? Using a simple rectangular mould and a mould-filling and cooling analysis (Moldflow), the place and thickness dependent thermal history can be computed everywhere in the mould, see Fig. 16a. Subsequently, it is assumed that the evolution of yield stress, during cooling from the melt to below $T_g$, is governed by the same evolution kinetics of the state parameter $S$, as observed during progressive aging, Fig. 10b. This enables us to translate the (local) thermal histories to (local) values of the state parameter $S$ and, with that, predict the distribution of yield stress over the sample [50], see Fig. 16b. As shown in Fig. 16c, the distribution of yield stress depends strongly on the mould temperature, that apart from the sample thickness is the key parameter determining the local cooling rate.

In Fig. 16d, the predictions are compared with experiments using different mould temperatures. The computed average yield stresses compare amazingly well with the experimentally determined values, the symbols in Fig. 16b. An extension of this results by modeling polymers other than PC, such as e.g. PS, PVC and later HDPE, is of our present research

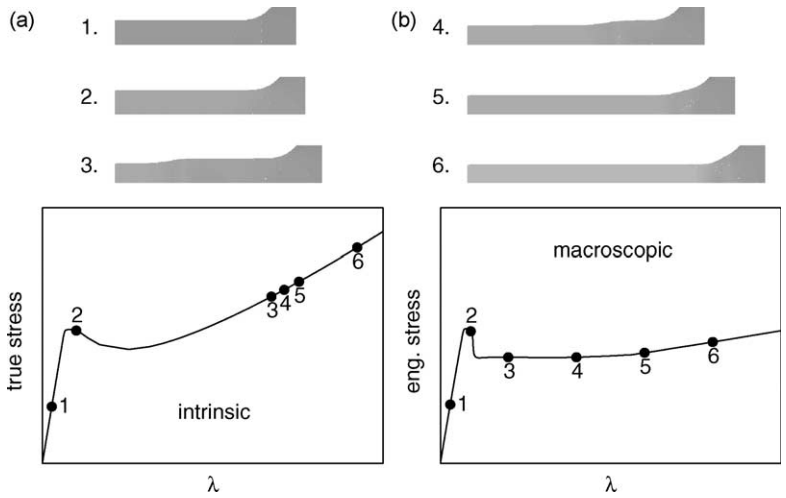


Fig. 13. Tensile testing of PC. From intrinsic to macroscopic behavior. We plot the true stress in the middle of the test bar (the neck, left) as a function of the local strain, (a), and the resulting engineering stress, which is the tensile force measured right at the clamping side over the initial cross-section of the test bar, versus engineering strain, defined as the length of the test bar over the original length, see (b), at six different stages of the test.

interest. Motivation is that this results clearly opens the possibility to predict a polymer's life time performance without performing a single mechanical test.

## 7. Craze initiation

Although interesting so far, the polymer story is not finished yet with the results obtained on the intrinsic behavior that can reversibly at wish be altered by physical ageing and mechanical rejuvenation. Neither are we finished after the quantification of the polymers response, using advanced constitutive equations that capture the physics appropriately and allow us to predict the polymer's future in dependence of its past given the transient stress and temperature profiles it will experience during use. First reason to continue the analysis is that if we scratch, e.g. bullet proof PC, upon impacting the material breaks brittle via crazing. Moreover, we also want to improve on brittle polymers like PS, to prevent them from crazing and introduce shear yielding. Crazing has been studied in great detail by a large number of experts from which Ed Kramer in Cornell, Itaca (now in Santa Barbara) was, without any doubt, the most original one.[10] He designed beautiful experiments and developed now well-established theories [51–59]. His general starting picture is that, *after plastic flow*, a craze develops via the initiation of a cavity, the growth of instabilities and finally the coalescence of holes. In order to tackle the problem here in a simple way, we will focus on the initiation of the first hole in the material, underneath a scratch or a surface defect. For that we need a craze-initiation criterion and to identify that we performed micro-indentation tests with a sphere of 250 μm pushed into the surface of quenched and annealed PS samples using different normal loads [60]. After the experiments

[10] At the occasion of the 50th anniversary celebration of the Journal of Polymer Science, the editors selected Henkee and Kramer's original break-through paper of 1984 [53] to be reprinted in 1996. It is still today interesting to read Ed Kramer's (and also Hugh Brown's) reflection written on this occasion [54]. Please taste the following sentence: 'Even today the idea that a linear viscoelastic measurement of the rubbery plateau modulus in the melt could elucidate the large strain plastic deformation behavior of the glass seems nothing short of miraculous; but there were certainly many hints in previous work that entanglements were important for both deformation and fracture'.

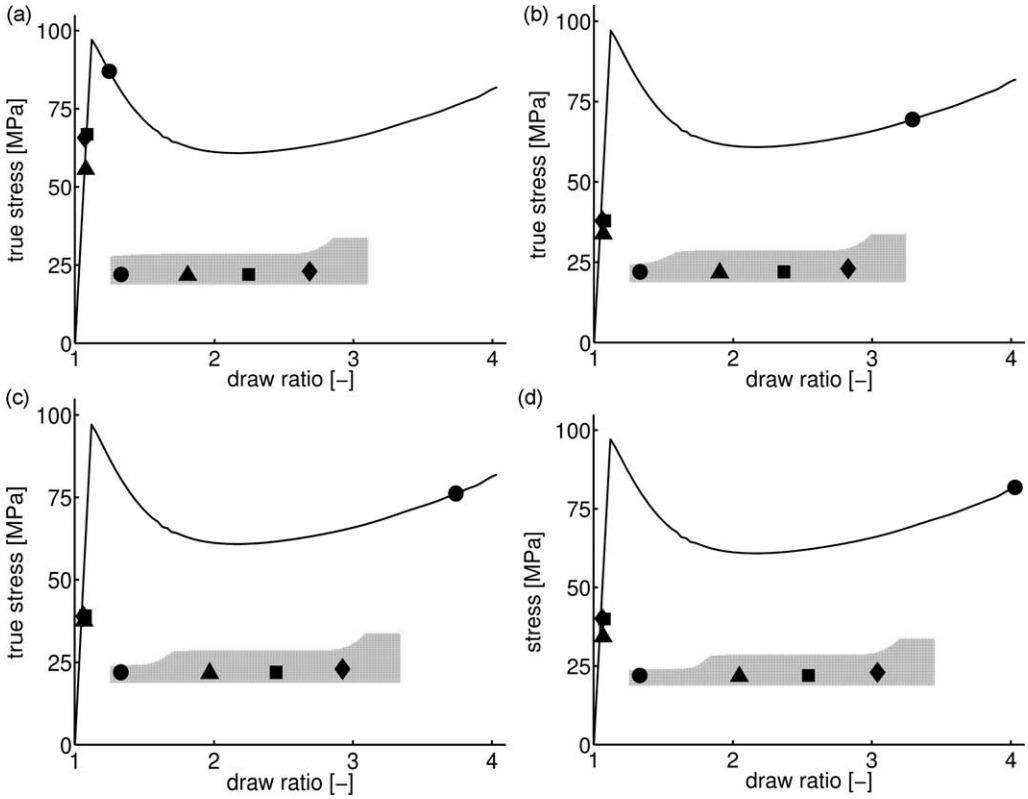


Fig. 14. Tensile testing of PS. After neck formation at yield strain softening sets in, the stress in the remaining part of the test bar decreases substantially due to unloading because of strain localization in the neck. Subsequently, strain hardening occurs in he neck, but it is insufficiently pronounced. Localization remains in the neck, until fibril failure there occurs.

we counted the number of (radial) crazes that were caused by indentation as a function of the load applied.

Extrapolating to zero crazes yielded critical normal forces of ca. 1.5 and 2.5 N, respectively. Performing numerical simulations of the same tests, using the advanced constitutive equations developed, we computed the maximum values of the maximum hydrostatic stress, somewhere in the sample, during

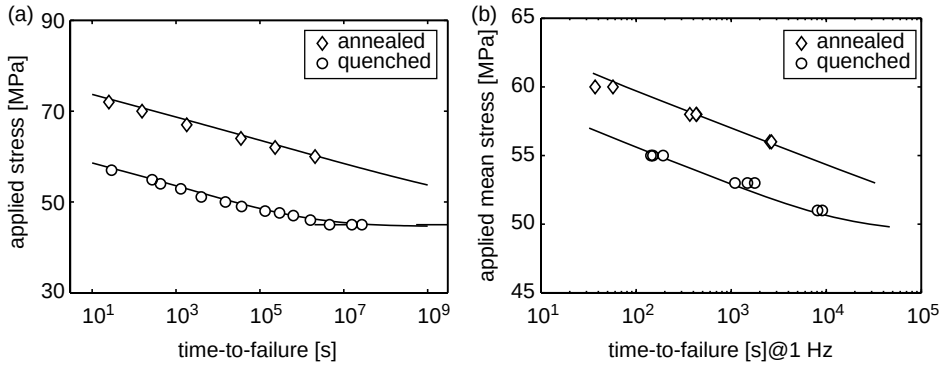


Fig. 15. Life time prediction of PC during creep loading (a) and fatigue loading (b) with symbols the experimental results and full lines the model predictions without any adjustable parameter [49].

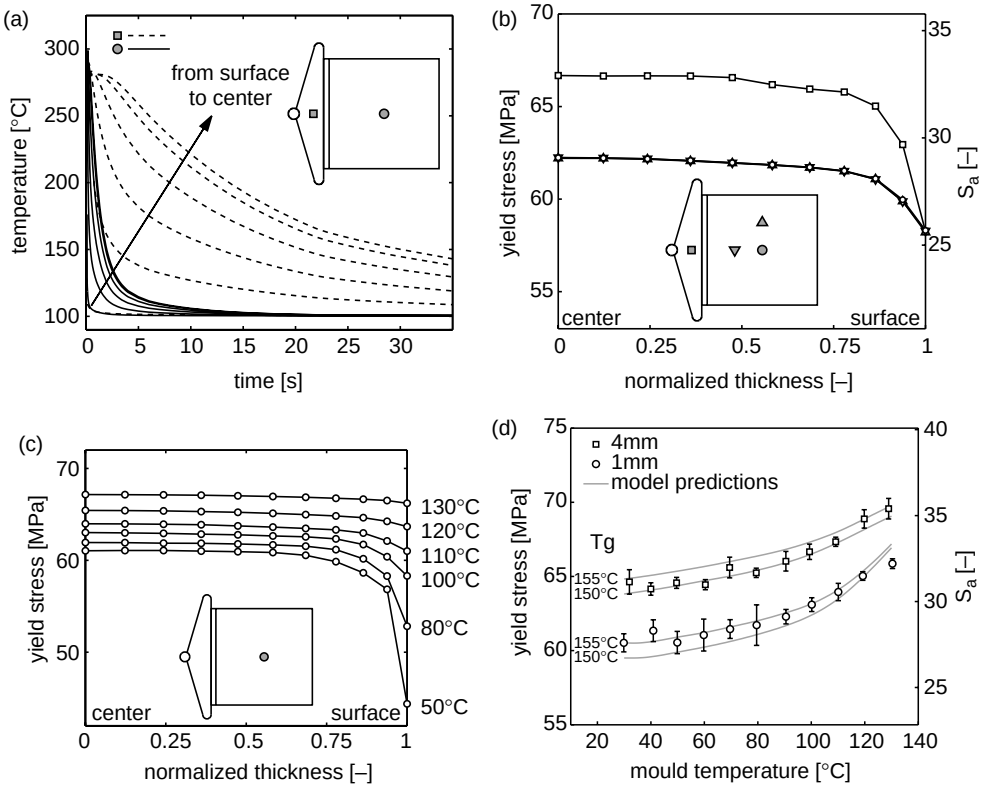


Fig. 16. Thermal history within a simple rectangular mould (a) and resulting calculated yield stress (b) and comparison of the averaged calculated and experimental yield stress as a function of mould temperature used during injection moulding (c and d).

loading as function of the normal force applied, see Fig. 17a. For both, the quenched and annealed samples, this leads to the same critical value for the hydrostatic stress for PS of 40 MPa, above which a cavity will form that will lead to the first craze. Performing the same test for different amorphous polymers, characterized by their entanglement density $\nu_e \sim 1/M_e$, resulted in a semi-log relation giving, e.g. for PC a critical value of 90 MPa, see Fig. 17b.

Using these critical values, finite element simulations can be performed on notched tensile bars, with a small defect under the notch representing the fresh cut of a quenched razor knife, see Fig. 18a.

Similar to the analysis of the micro-indentation tests, we can compute the maximum hydrostatic stress, somewhere in the sample, during loading. We find cavity formation and thus craze initiation in PS under the defect at low macroscopic strains [61], see Fig. 18b, while PC survives this problem but exceeds the critical hydrostatic stress of 90 MPa under the notch at a macroscopic strain of ca. 1%, see Fig. 18c. It is because of these problems that polymers need to be made heterogeneous, e.g. by rubber modification. What the heterogeneity (soft inclusions into the glassy matrix) typically should taken care of is to prevent the critical distance to occur everywhere in the glassy matrix, such that the tri-axial stress state can not exist, thus crazing can not start. The typical distance in PS is very small, see Fig. 18b, and is given by the distance from the surface to the place where the maximum hydrostatic stress is found. Although FEM calculations bear no absolute dimensions, Robert Smit took experiments as his starting point in modeling and based thereupon, this distance could be very roughly estimated using the amplitude of the defect, to be $\ll$ 1 μm, while for PC the critical distance could be

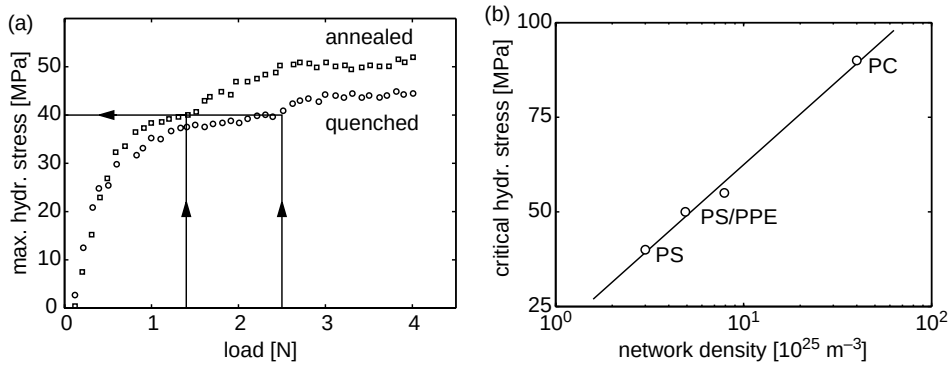


Fig. 17. Maximum hydrostatic stress in the sample during micro-indentation for quenched and annealed PS (a) and entanglement density dependence of the critical value of this stress (b).

estimated using the curvature of the notch to be $\ll$ 200 μm [61].

## 8. Heterogeneous systems

So, although critical distances apparently differ for different polymers, characterized by the ratio of strain hardening and strain softening after yield, the need for heterogeneity is universal and its role is to prevent the first cavity of the first craze to start to grow. Although in practice usually rubber is used as impact modifier, we will start the analysis with a zero modulus rubber, holes, that should prevent the critical triaxial stress state to occur. The problems met in analyzing heterogeneous polymer systems were threefold: (i) the complex behavior of the constituents, (ii) the complex geometry of the microstructure, and (iii) the unknown relation between micro events and macroscopic behavior. The first problem was solved after the development of reliable 3D quantitative constitutive equations, see Table 1, the second problem by using FEM, finite element methods, and for the last problem we developed the MLFEM, multi-level finite element model [62–66]. Basically, MLFEM uses a FEM analysis of the macroscopic structure and goes one level down in every integration point of every finite element. The local displacements in these integration points are enforced on the edges of bi-periodic RVE's, representative volume elements, see Fig. 19.

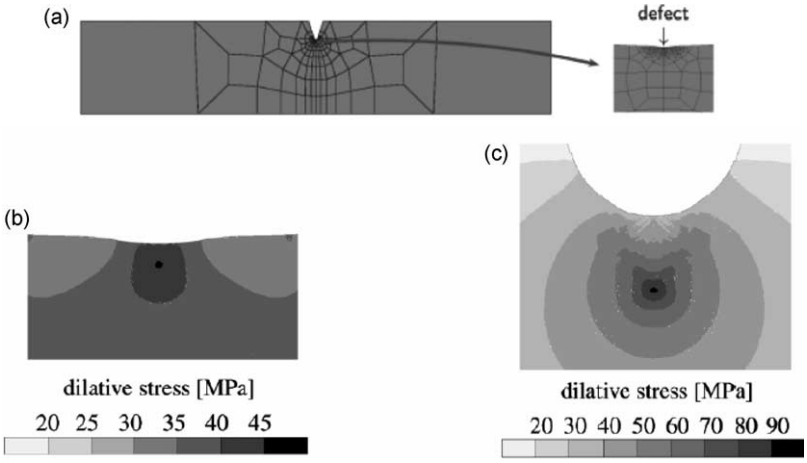


Fig. 18. Meshed notched tensile bar with defect under the notch (a). Resulting stress profiles during loading, showing that the critical hydrostatic stress of 40 MPa is reach for PS underneath the defect already at low macroscopic strains of $<0.2\%$ (b) while for PC, that survives the defect sensitivity, the critical hydrostatic stress of 90 MPa is reached below the notch at a macroscopic strain of ca. 1% (c) [61].

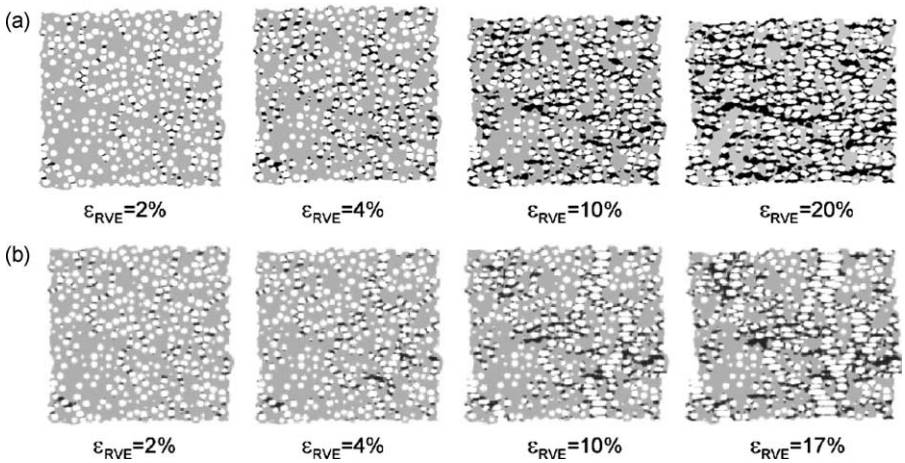


Fig. 19. Loading representative volume elements, RVE's, of PC (a) and PS (b). Gray is below yield, black represents places that are plastically deformed [64].

The RVE's are meshed and loaded, after which the average RVE stress is computed and brought back to the highest FEM level, to solve the balance equations. The procedure repeats, until equilibrium is reached. Then the next incremental strain step is applied. In this way we use the RVE analysis as a non-closed form of a constitutive equation for the complex microstructure. Besides, a local check inside every RVE on local failure is possible [87]. Fig. 19 compares the RVE responses of PC, Fig. 19a, and PS, Fig. 19b, discriminating between elastically loaded and plastically deformed regions. Of course already at extremely low macroscopic strains, localizations set in, there where two holes are accidentally close such that a stress concentration exists. The material starts to locally flow. In contrast to PC, that eventually spreads plastic deformation over the total RVE, in PS it still localizes in bands perpendicular to the loading direction, Fig. 19b.

Reason is the lack of strain hardening in PS, given its low entanglement density $\nu_e$ or high molecular weight between entanglements $M_e$, caused by its large chain stiffness. As in Fig. 14, we again can conclude via this RVE-analysis that PS is indeed too ductile to be tough. The thin filaments formed are not able to transfer load and strain keeps localized until the fibrils break. The consequences of this RVE response are clearly found on the macro-level when applying MLFEM, see Fig. 20.

PC that homogeneously hits the 90 MPa hydrostatic stress criterion at low macroscopic strains, Fig. 20b, is completely tough in the heterogeneous case, Fig. 20d. In Fig. 20, 30% voids were used, but also 5% voids prove to be sufficient for PC [65]. This illustrates that it is quite easy to toughen PC. PS on the contrary hits in its homogeneous state the 40 MPa criterion already at very low strains, Fig. 20a, but only slightly improves when made heterogeneous, Fig. 20c. Although clearly improved and comparable with plain PC, the deformation still localizes in a band perpendicular to the drawing direction and eventually the filaments in the RVE will break, see also Fig. 19b.

## 9. Optimal toughness modifier

Apparently for too ductile, too easy to flow, polymers like PS, we need to do a little bit more. In order to increase strain hardening, since that is what we need, we can introduce a smaller $M_e$ by mixing PS with PPE, which is the miscible Noryl® blend of GEP see Fig. 11, or alternatively chemically crosslinked PS [53].

A more practical way is to let a rubber shell locally support the straining filaments, not changing the PS properties, but changing the local structure properties to make it more strain-hardening, see Fig. 21. This now seems to be successful. PS is

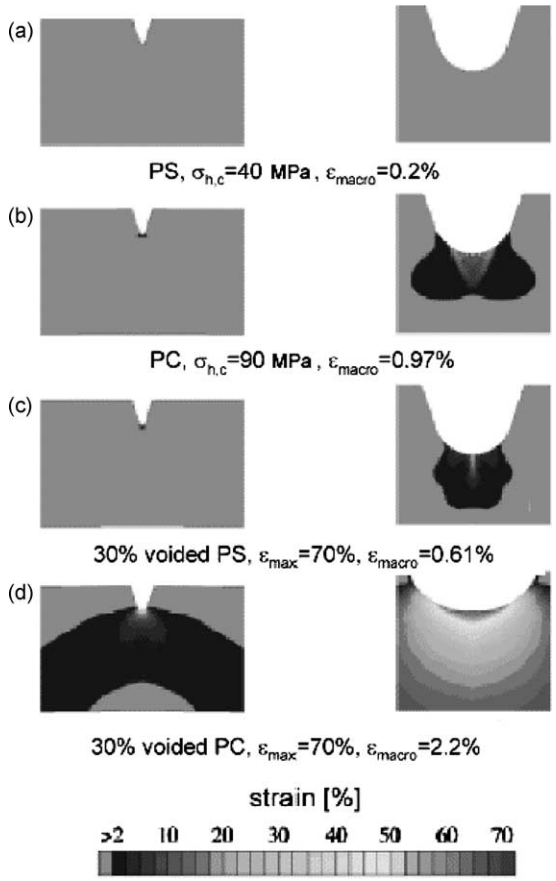


Fig. 20. MLFEM results on loading a notched, scratched tensile bar of homogeneous and heterogeneous (30% voids) PC (b and d), and PS (a and c). Strain localizations and delocalizations are shown, explaining the toughness of these two extreme polymers [65].

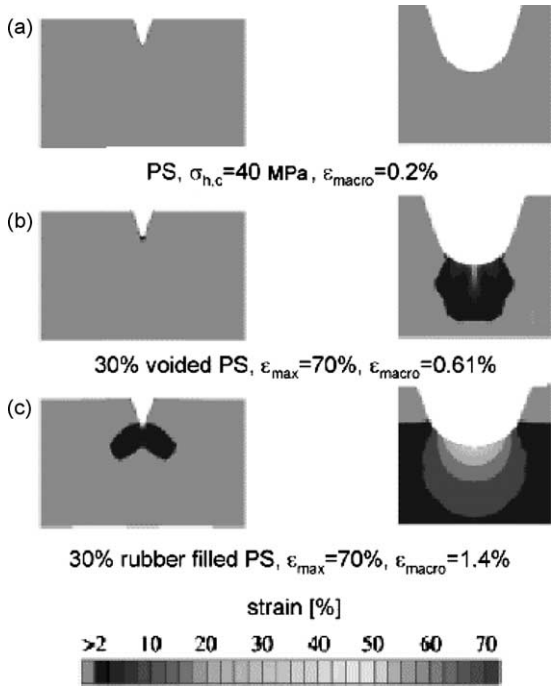


Fig. 21. MLFEM results on loading a notched, scratched tensile bar of homogeneous (a) and heterogeneous PS with 30% voids (b) or with 30% precavitated rubber particles supporting the filaments (c). Only in the last case delocalization of strain is found and toughness is obtained [65].

tough. During loading we did not meet a failure criterion and it was only since we had to remesh on the RVE level that we had to stop the computation. The idea of precavitation of the rubber particles is based on the fact that we do not want to rely on the in situ cavitating capabilities of the rubbery particles during impact loading under low temperatures [67–72]. The last two conditions basically increase the glass transition temperature of the rubber, making it more and more difficult to cavitate, which is necessary to prevent the occurrence of too high tri-axial stresses. (If we let the material self decide where to cavitate, it will form one localized craze in the plane perpendicular to the loading direction, making the polymer brittle.) Besides low temperatures and high deformation rates, we moreover want to apply extremely small particles of the impact modifiers used, despite that they are difficult to cavitate. Reason is that we than need less rubber, so modulus and yield stress remain high, but also that we still can keep optical clarity. An illustrative example is found in Fig. 22 where for an in situ copolymerized PMMA–aliphatic epoxy system (80–20) with 30 nm dispersed phase, impact toughness is found, only after precavitating the samples at low deformation rates [73–76].

A second example of precavitating rubber inclusions can be found in Clive Bucknalls work, using thermal contraction tests where he supercooled heterogeneous polymer systems for sufficiently long times to induce rubber cavitation [77,78]. As a result, experiments and simulations suggest that the universal optimal impact modifier is a 3000–300–30–3 system with in a matrix of 3000 MPa (all amorphous

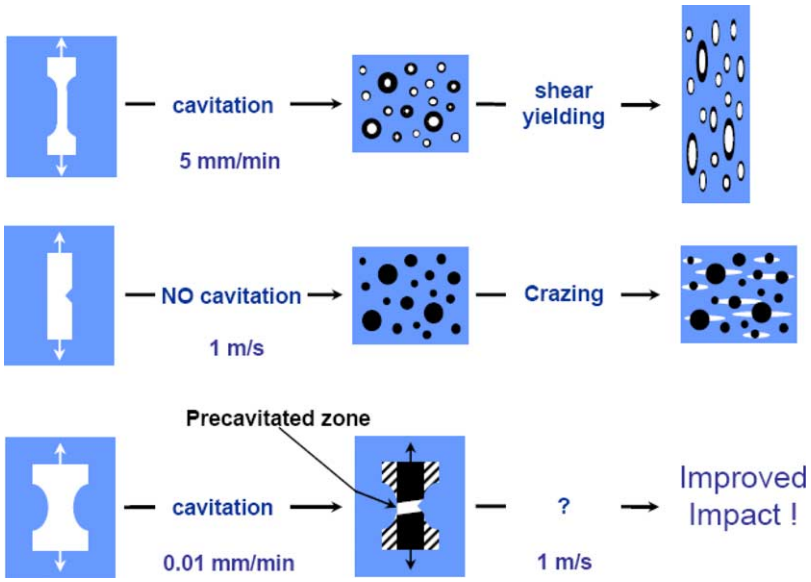


Fig. 22. In situ X ray experiments on a PMMA–aliphatic epoxy system during slow and fast loading [75].

polymers) we add a 30 nm dispersion of a precavitated core-shell rubber with a shell with a pretty high rubber modulus of 300 MPa and a core that should be a hole, so with a modulus $\ll 3$ MPa. We tried to make these structures via a CIPS process, chemically induced phase separation, making use of a self-organizing process in diblock copolymers [79–82]. Nanostructures were induced and in PS/PBA–PEB 75-25 blends with poly-butylacrylate as a rubber shell and polyethylene-(co)butylene as the liquid core, a change from crazing to cavitation-induced shear yielding was found [79,80] while the macroscopic strain of the triblock system PMMA–PBA–PEB proved to increase to 140% [81]. Using a crystallizable polymer as a core, also cavitation can be obtained as was proven by the system PS–PB–PCL, where polybutene was the shell of the dispersed phase and polycaprolacton the crystallizing core [82]. In all cases, we still needed a too large amount of impact modifier. The first one to prove that an optimal impact modifier indeed can be realized was Christian Koulic from Jerome's Liege group [83–86] who found that cucumber-type of structures of PS-PIP in PA, with a size of around 50 nm, gave maximum toughness with only 4% rubber added, see Fig. 23.

## 10. Brittle-to-tough transitions

Finally, if we apply the craze initiation criterion used in Sections 6–8, on the deformation of heterogeneous systems, we can find both a temperature induced brittle-to-tough transition, see Fig. 24a, as well as a critical interparticle distance induced transition, see Fig. 24b [87].

The critical interparticle distance originates from the fact that the $T_g$ of a polymer decreases at a surface (and increases at a solid interface) over a depth of 100 nm [88–91]. As a consequence, $T_g$ is at room temperature at the surface and reaches its bulk value only at 100 nm. As a result, the near-surface mechanical properties are different from that in the bulk [92]. This now gives an absolute scale in the microstructure, but also in the finite element calculations, where we replace a change in $T_g$ by a change in temperature from the surface into the bulk, gradually changing over the same 100 nm. The size of the (constant volume fraction) dispersed phase now determines whether or not this layer of lower $T_g$, thus lower yield stress $\sigma_y$ percolates

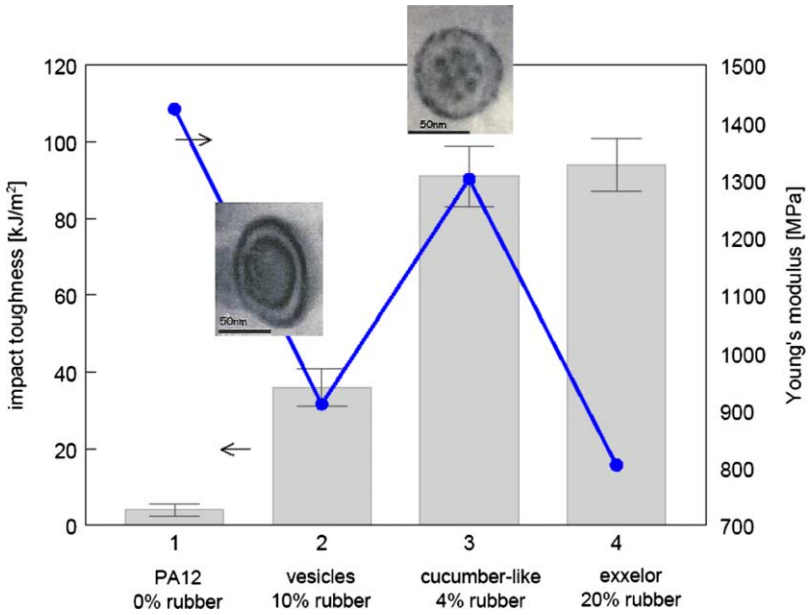


Fig. 23. Rubber toughened polyamide demonstrating the existence of the optimal impact modifier [83–86].

through the RVE yes or no, thereby determining toughness.

## 11. Conclusions

The major conclusions to be drawn are that (i) toughness is equivalent to delocalization of strain, (ii) the two types of bonds present make all polymers intrinsically tough, (iii) polystyrene is too ductile to be tough (but supporting shells increase strain hardening of the local structure), (iv) proper constitutive modeling enables to quantitatively describe polymer responses, including the effects of temperature, strain rate, and time (ageing), (v) an independent craze initiation criterion must be added in order to numerically predict failure and this criterion can be experimentally determined by using indentation tests, (vi) all polymers must be made heterogeneous in order to circumvent defect or notch sensitivity, (vii)

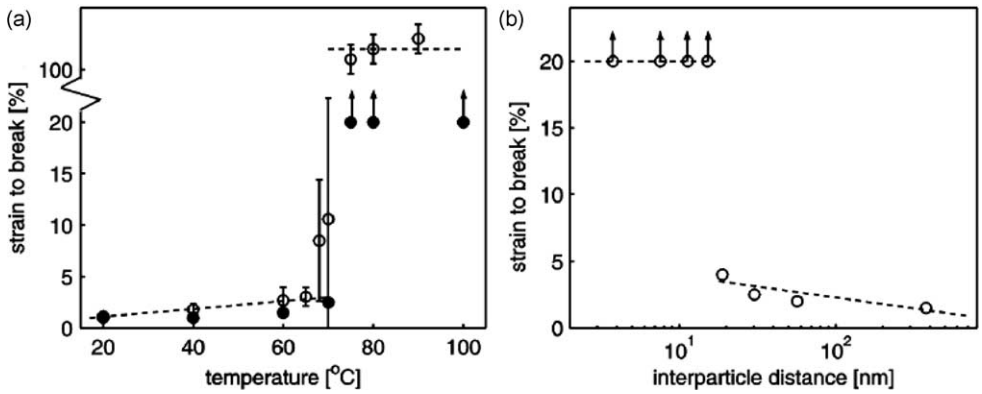


Fig. 24. *B–T* transitions for heterogeneous PS as a function of temperature (a), and critical interparticle distance (b) [87].

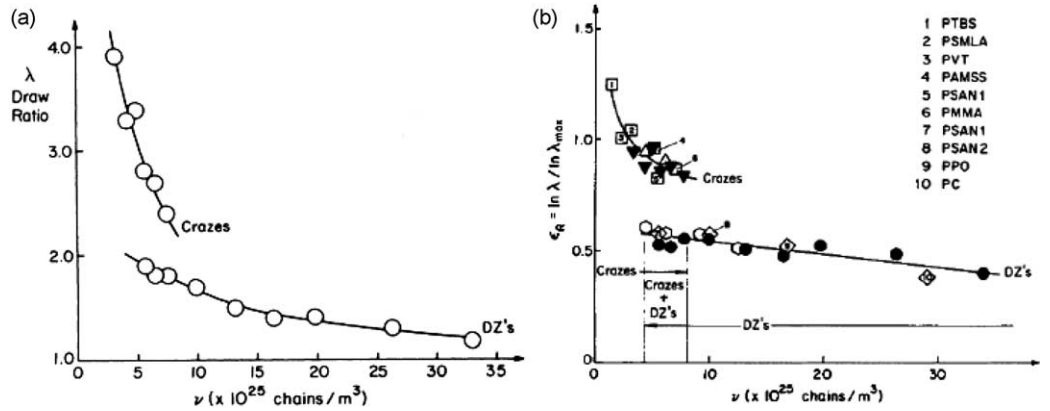


Fig. 25. Extension ratio in crazes and deformation zones (DZ's) as a function of network density $\nu$ ($\sim 1/M_e$) in (un)crosslinked PS films (a). Similar plot for different polymers (PPO is the somewhat confusing old notation for poly-phenylene-ether, PPE) (b). Reproduced with permission from [53].

modeling suggests that the ultimate toughness modifier is a 3–30–300–3000 pre-cavitated core-shell rubber with core $\ll$3 MPa modulus, 30 nm diameter, shell 300 MPa modulus in a matrix of 3000 MPa, and finally (viii) modeling suggests the presence of both a temperature induced as well as a critical interparticle distance induced brittle-to-tough transition in polymeric materials.

How do the present analyses cope with the previously empirically determined relation between chain stiffness and molecular weight between entanglements [93,94] and its relation with drawability and the transition from crazing to shear yielding [53–59], see Fig. 25.

The answer is straightforward. On the one hand, the strain hardening modulus proves to be directly related to $M_e$, while a larger modulus gives less strain softening thus less localization changing the deformation behavior from crazing to shear yielding, see Figs. 11–14. On the other hand, there exists a relation between the critical stress for craze initiation and $M_e$, see Fig. 17b, making the higher entangled polymers less sensitive for scratches and easier to rubber modify, see Figs. 18–21.

## Acknowledgements

This paper is based on a number of successive and ongoing PhD studies in our group: Marco van der Sanden (1993) on the concept of ultimate toughness, Theo Tervoort (1996) on constitutive modeling, Peter Timmermans (1997) on modeling of necking, Robert Smit (1998) on the multi-level finite element method, Bernd Jansen (1998) on microstructures for ultimate toughness, Harold van Melick (2002) on quantitative modeling, Bernard Schrauwen (2003) on semi-crystalline polymers, Hans van Dommelen (2003) on multi-scale semi-crystalline, Ilse van Casteren (2003) on nanostructures for ultimate toughness, Edwin Klompen (2005) on long-term prediction, Jules Kierkels (2006) on toughness in films, Roel Janssen (2006) on creep rupture and fatigue, and Tom Engels (2007) on coupling of processing with properties. Theses are downloadable from (please select by year) http://www.mate.tue.nl/mate/publications/index.php/4. The research was sponsored by the Dutch Polymer Insitute, DPI, the national science foundation, STW, and the university, TU/e.

## References

[1] G'Sell C, Jonas JJ. Yield and transient effects during the plastic deformation of solid polymers. J Mater Sci 1981;16(7):1956–74.

[2] G'Sell C, Hiver JM, Dahoun A, Souahi A. Video-controlled tensile testing of polymers and metals beyond the necking point. J Mater Sci 1992;27(18):5031–9.

[3] Arruda EM, Boyce MC. Evolution of plastic anisotropy in amorphous polymers during finite straining. Int J Plast 1993;9(6):697–720.

[4] Boyce MC, Arruda EM, Jayachandran R. The large strain compression, tension, and simple shear of polycarbonate. Polym Eng Sci 1994;34(9):716–25.
[5] McLeish TCB, Milner ST. Entangled dynamics and melt flow of branched polymers. Adv Polym Sci 1999;143(Branched Polymers II):195–256.
[6] Read DJ, McLeish TCB. Molecular rheology and statistics of long chain branched metallocene-catalyzed polyolefins. Macromolecules 2001;34(6):1928–45.
[7] Swartjes FHM, Peters GWM, Rastogi S, Meijer HEH. Stress induced crystallization in elongational flow. Int Polym Proc 2003;18(1):53–66.
[8] Tervoort TA, Visjager JF, Smith P. Melt-processable poly(tetrafluoroethylene)-compounding, fillers and dyes. J Fluorine Chem 2002;114(2):133–7.
[9] Tervoort TA, Visjager JF, Graf B, Smith P. Melt-processable poly(tetrafluoroethylene). Macromolecules 2000;33(17): 6460–5.
[10] Tervoort TA, Visjager JF, Smith P. On abrasive wear of polyethylene. Macromolecules 2002;35(22):8467–71.
[11] Smith P, Lemstra PJ, Kalb B, Pennings AJ. Ultrahigh-strength polyethylene filaments by solution spinning and hot drawing. Polym Bull 1979;1(11):733–6.
[12] Smith P, Lemstra PJ. Ultrahigh-strength polyethylene filaments by solution spinning/drawing. 2. Influence of solvent on the drawability. Makromolekulare Chemie 1979;180(12): 2983–6.
[13] Smith P, Lemstra PJ. Ultrahigh strength polyethylene filaments by solution spinning/drawing. 3. Influence of drawing temperature. Polymer 1980;21(11):1341–3.
[14] Kwolek SL, US Patent 3671 542; 1972.
[15] Yang HH. Aromatic high-strength fibers. New York: Wiley; 1989.
[16] Gordon JE. Structures, or why things don't fall down.: Da Capo Press; 1978 p. 74.
[17] Clyne TW, Phillipps AJ. Interfacial control and macroscopic failure in long-fiber-reinforced and laminated inorganic composites. Comp Sci Tech 1994;51(2):271–82.
[18] Smith BL, Schaffer TE, Viani M, Thompson JB, Frederick NA, Kind J, et al. Molecular mechanistic origin of the toughness of natural adhesives, fibers and composites. Nature 1999;399(6738):761–3.
[19] Wang RZ, Suo Z, Evans AG, Yao N, Aksay IA. Deformation mechanisms in nacre. J Mater Res 2001;16(9):2485–93.
[20] Haward RN, Thackray G. Use of a mathematical model to describe isothermal stress-strain curves in glassy thermoplastics. Proc R Soc London Ser A 1967;302(1471):453–72.
[21] Govaert LE. Bob Haward, a chemist on the quest for strength. J Polym Sci Part B 2004;42(11):iii–iiv.
[22] Boyce MC, Parks DM, Argon AS. Mech Mater 1988;7: 15–33.
[23] Hasan OA, Boyce MC. A constitutive model for the nonlinear viscoelastic viscoplastic behaviour of glassy polymers. Polym Eng Sci 1995;35:331–44.
[24] Buckley CP, Jones DC. Glass-rubber constitutive model for amorphous polymers near the glass transition. Polymer 1995; 36:3301–12.
[25] Dooling PJ, Buckley CP, Hinduja S. The onset of nonlinear viscoelasticity in multiaxial creep of glassy polymers: a constitutive model and its application to PMMA. Polym Eng Sci 1998;38:892–904.
[26] Gerlach C, Buckley CP, Jones DP. Development of an integrated approach to modelling of polymer film orientation processes. Trans Inst Chem Eng Part A 1998;76:38–44.
[27] Tervoort TA, Klompen ETJ, Govaert LE. A multi-mode approach to finite, three-dimensional, nonlinear viscoelastic behaviour of polymer glasses. J Rheol 1996;40: 779–97.
[28] Govaert LE, Timmermans PHM, Brekelmans WAM. The influence of intrinsic strain softening on strain localisation in polycarbonate: modeling and experimental validation. J Eng Mater Technol 2000;122:177–85.
[29] Klompen ETJ, Engels TAP, Govaert LE, Meijer HEH. Modelling of the post-yield response of glassy polymers: influence of thermomechanical history. Macromolecules 2005, 38(16):6997–7008.
[30] Loo LS, Cohen RE, Gleason KK. Chain mobility in the amorphous region of nylon 6 observed under active uniaxial deformation. Science 2000;288(5463):116–9.
[31] Capaldi FM, Boyce MC, Rutledge GC. Enhanced mobility accompanies the active deformation of a glassy amorphous polymer. Phys Rev Lett 2002;89(17):175505.
[32] Theodorou DN, Suter UW. Local structure and the mechanism of response to elastic deformation in a glassy polymer. Macromolecules 1986;19(2):379–87.
[33] van Melick HGH, Govaert LE, Meijer HEH. Localization phenomena in glassy polymers: influence of thermal and mechanical history. Polymer 2003;44(12):3579–91.
[34] McKenna GB. Mechanical rejuvenation in polymer glasses: fact or fallacy? J Phys Cond Matter 2003;15(11):S737–S63.
[35] Tervoort TA, Govaert LE. Strain-hardening behavior of polycarbonate in the glassy state. J Rheol 2000;44(6): 1263–77.
[36] Govaert LE, van Melick HGH, Meijer HEH. Temporary toughening of polystyrene through mechanical pre-conditioning. Polymer 2001;42(3):1271–4.
[37] van Melick HGH, Govaert LE, Raas B, Nauta WJ, Meijer HEH. Kinetics of ageing and re-embrittlement of mechanically rejuvenated polystyrene. Polymer 2003;44(4): 1171–9.
[38] Struik LCE. Private communications.
[39] Hodge IM. Enthalpy relaxation and recovery in amorphous materials. J Non-Cryst Solid 1994;169:211–66.
[40] Hutchinson JM. Physical aging of polymers. Prog Polym Sci 1995;20:703–60.
[41] Struik LCE. Physical ageing of amorphous polymers and other materials. Amsterdam: Elsevier; 1978.
[42] Aref-Azar A, Biddlestone F, Hay JN, Haward RN. The effect of physical ageing on the properties of poly(ethylene terephthalate). Polymer 1983;24(10):1245–51.
[43] Utz M, Debenedetti PG, Stillinger FH. Atomistic simulation of aging and rejuvenation in glasses. Phys Rev Lett 2000;84(7): 1471–4.

[44] Nandagopal M, Utz M. Thermal versus deformation-induced relaxation in a glass-forming fluid. J Chem Phys 2003; 118(18):8373–7.
[45] Lei Y, Cummins K, Lacks DJ. First-principles enthalpy landscape analysis of structural recovery in glasses. J Polym Sci, Part B 2003;41(19):2302–6.
[46] Lacks DJ, Osborne MJ. Energy landscape picture of overaging and rejuvenation in a sheared glass. Phys Rev Lett 2004; 93(25):255501/1–255501/4.
[47] Wu JJ, Buckley CP. Plastic deformation of glassy polystyrene: A unified model of yield and the role of chain length. J Polym Sci Part B 2004;42(11):2027–40.
[48] van Melick HGH, Govaert LE, Meijer HEH. On the origin of strain hardening in glassy polymers. Polymer 2003;44(8): 2493–502.
[49] Klompen ETJ, Govaert LE, Engels TAP, van Breemen LCA, Schreurs PJG, Meijer HEH. Quantitative prediction of long-term failure in polycarbonate, Macromolecules 2005;38(16): 7009–17.
[50] Govaert LE, Engels TAP, Klompen ETJ, Peters GWM, Meijer HEH. Processing induced properties of glassy polymers: yield stress development in polycarbonate. Int Polym Proc 2005; 20(2):170–7.
[51] Kramer EJ. Microscopic and molecular fundamentals of crazing. Adv Polym Sci 1983;52–53:1–56.
[52] Kramer EJ, Berger LL. Fundamental processes of craze growth and fracture. Adv Polym Sci 1990;91/92:1–68 [Crazing Polym., Vol. 2].
[53] Henkee CS, Kramer EJ. Crazing and shear deformation in crosslinked polystyrene. J Polym Sci, Polym Phys Ed 1996; 22(4):721–37. Reprinted from J Polym Sci, Part B 1996;34(17) 2825–41.
[54] Kramer EJ. Reflections on "Crazing and shear deformation in crosslinked polystyrene," by Chris S. Henkee, Edward J. Kramer. J Polym Sci, Polym Phys Ed, 1984;22:721. Comment. J Polym Sci, Part B 1996:34(17) 2821–22.
[55] Donald AM, Kramer EJ. The mechanism for craze-tip advance in glassy polymers. Philos Mag A 1981;43(4):857–70.
[56] Donald AM, Kramer EJ. Plane stress deformation zones at crack tips in polycarbonate. J Mater Sci 1981;16(11): 2967–76.
[57] Donald AM, Kramer EJ. Effect of molecular entanglements on craze microstructure in glassy polymers. J Polym Sci, Polym Phys Ed 1982;20(5):899–909.
[58] Donald AM, Kramer EJ. Deformation zones and entanglements in glassy polymers. Polymer 1982;23(8):1183–8.
[59] Donald AM, Kramer EJ, Kambour RP. Interaction of crazes with preexisting shear bands in glassy polymers. J Mater Sci 1982;17(6):1739–44.
[60] Van Melick HGH, Bressers OFJT, Den Toonder JMJ, Govaert LE, Meijer HEH. A micro-indentation method for probing the craze-initiation stress in glassy polymers. Polymer 2003;44(8):2481–91.
[61] Smit RJM, Brekelmans WAM, Meijer HEH. Predictive modelling of the properties and toughness of polymeric materials. Part I. Why is polystyrene brittle and polycarbonate tough? J Mater Sci 2000;35(11):2855–67.
[62] Smit RJM, Brekelmans WAM, Meijer HEH. Prediction of the mechanical behavior of nonlinear heterogeneous systems by multilevel finite element modeling. Comput Methods Appl Mech Eng 1998;155:181–92.
[63] Smit RJM, Brekelmans WAM, Meijer HEH. Prediction of the large-strain mechanical response of heterogeneous polymer systems: local and global deformation behavior of a representative volume element of voided polycarbonate. J Mech Phys Solid 1999;47(2):201–21.
[64] Smit RJM, Brekelmans WAM, Meijer HEH. Predictive modelling of the properties and toughness of polymeric materials. Part II. Effect of microstructural properties on the macroscopic response of rubber-modified polymers. J Mater Sci 2000;35(11):2869–79.
[65] Smit RJM, Brekelmans WAM, Meijer HEH. Predictive modelling of the properties and toughness of polymeric materials part III simultaneous prediction of micro- and macrostructural deformation of rubber-modified polymers. J Mater Sci 2000;35(11):2881–92.
[66] Meijer HEH, Govaert LE, Smit RJM. A multi-level finite element method for modeling rubber-toughened amorphous polymers. ACS Symp Ser 2000;759(Toughening of Plastics): 50–70.
[67] Bucknall CB, Karpodinis A, Zhang XC. A model for particle cavitation in rubber-toughened plastics. J Mater Sci 1994; 29(13):3377–83.
[68] Ayre DS, Bucknall CB. Particle cavitation in rubber-toughened PMMA: experimental testing of the energy-balance criterion. Polymer 1998;39(20):4785–91.
[69] Lin CS, Ayre DS, Bucknall CB. A dynamic mechanical technique for detecting rubber particle cavitation in toughened plastics. J Mater Sci Lett 1998;17(8):669–71.
[70] Bucknall CB, Rizzieri R, Moore DR. Detection of incipient rubber particle cavitation in toughened PMMA using dynamic mechanical tests. Polymer 2000;41(11):4149–56.
[71] Lazzeri A, Bucknall CB. Recent developments in the modeling of dilatational yielding in toughened plastics. ACS Symp Ser 2000;759(Toughening of Plastics):14–35.
[72] Bucknall CB. Blends containing core-shell impact modifiers part 1. Structure and tensile deformation mechanisms. Pure Appl Chem 2001;73(6):897–912.
[73] Jansen BJP, Rastogi S, Meijer HEH, Lemstra PJ. Rubber-modified glassy amorphous polymers prepared via chemically induced phase separation. 1. Morphology development and mechanical properties. Macromolecules 2001;34(12): 3998–4006.
[74] Jansen BJP, Rastogi S, Meijer HEH, Lemstra PJ. Rubber-modified glassy amorphous polymers prepared via chemically induced phase separation. 2. Mode of microscopic deformation studied by in-situ small-angle X-ray scattering during tensile deformation. Macromolecules 2001;34(12): 4007–18.
[75] Jansen BJP, Rastogi S, Meijer HEH, Lemstra PJ. Rubber-modified glassy amorphous polymers prepared via chemically induced phase separation. 3. Influence of the strain rate on the microscopic deformation mechanism. Macromolecules 1999; 32(19):6283–9.

[76] Jansen BJP, Rastogi S, Meijer HEH, Lemstra PJ. Rubber-modified glassy amorphous polymers prepared via chemically induced phase separation. 4. Comparison of properties of semi- and full-IPNs, and copolymers of acrylate-aliphatic epoxy systems. Macromolecules 1999; 32(19):6290–7.
[77] Bucknall CB, Ayre DS, Dijkstra DJ. Detection of rubber particle cavitation in toughened plastics using thermal contraction tests. Polymer 2000;41(15):5937–47.
[78] Bucknall CB, Rizzieri R, Moore DR. Detection of cavitation in rubber phase of rubber toughened poly(methyl methacrylate) using thermal contraction measurements. Plast Rub Comp 2001;30(4):183–9.
[79] Van Casteren IA, Van Trier RAM, Goossens JGP, Meijer HEH, Lemstra PJ. The influence of hydrogen bonding on the preparation and mechanical properties of PS-diblock copolymer blends. J Polym Sci, Part B 2004;42(11): 2137–60.
[80] van Asselen OLJ, van Casteren IA, Goossens JGP, Meijer HEH. Deformation behavior of triblock copolymers based on polystyrene: an FT-IR spectroscopy study. Macromol Symp 2004;205(Polymer Spectroscopy):85–94.
[81] Van Casteren IA. Control of microstructures to induce ductility in brittle amorphous polymers. Dissertation Eindhoven University of Technology; 2003. p. 103–14 [chapter 6] (download at http://www.mate.tue.nl/mate/pdfs/3220.pdf).
[82] Van Casteren IA. Control of microstructures to induce ductility in brittle amorphous polymers. Dissertation Eindhoven University of Technology; 2003. p. 115–38 [chapter 7] (download at http://www.mate.tue.nl/mate/pdfs/3220.pdf).
[83] Koulic C, Jerome R. Nanostructure PMMA: from lamellar sheets to double-layered vesicles. Macromolecules 2004; 37(3):888–93.
[84] Koulic C, Jerome R. Nanostructured polyamide by reactive blending. 1. Effect of the reactive diblock composition. Macromolecules 2004;37(9):3459–69.
[85] Koulic C, Jerome R. Nanostructured polyamide by reactive blending: 2. Transition from nanovesicles to cucumber-like core-shell nano objects. Prog Colloid Polym Sci 2004;129: 70–5.
[86] Koulic C. Reactive blending as a tool towards nanostructured polymers. Dissertation University of Liège; 2004. p. 85–96 [chapter 5].
[87] van Melick HGH, Govaert LE, Meijer HEH. Prediction of brittle-to-ductile transitions in polystyrene. Polymer 2003; 44(2):457–65.
[88] Forrest JA, Mattsson j. Reductions of the glass transition temperature in thin polymer films: probing the length scale of cooperative dynamics. Phys Rev E 2000;61(1): R53–R6.
[89] Long D, Sotta P. How the shift of the glass transition temperature of thin polymer films depends on the adsorption with the substrate Los Alamos National Laboratory, Preprint Archive, Condensed Matter 2003:arXiv:cond-mat/0301100 2003 p. 1–33.
[90] Sotta P, Long D. The crossover from 2D to 3D percolation and its relationship to glass transition in thin films. Theory and numerical simulations Los Alamos National Laboratory, Preprint Archive, Condensed Matter 2003:arXiv:cond-mat/0301120 2003 p. 1–15.
[91] van Zanten JH, Wallace WE, Wu W-L. Effect of strongly favorable substrate interactions on the thermal properties of ultrathin polymer films. Phys Rev E 1996;53(3): R2053–R6.
[92] van Melick HGH, van Dijken A, den Toonder JMJ, Govaert LE, Meijer HEH. Near-surface mechanical properties of amorphous polymers. Philos Mag A 2002;82(10): 2093–102.
[93] Wu S. Chain structure and entanglement. J Polym Sci, Part B 1989;27(4):723–41.
[94] Wu S. Chain structure, phase morphology, and toughness relationships in polymers and blends. Polym Eng Sci 1990; 30(13):753–61.